Journal

Structure-Dependent Microwave Dielectric Properties and Middle-Temperature Sintering of Forsterite $(Mg_{1-x}Ni_x)_2SiO_4$ Ceramics

Chen Zhang, Ruzhong Zuo,[†] Jian Zhang, and Yang Wang

Institute of Electro Ceramics & Devices, School of Materials Science and Engineering, Hefei University of Technology, Hefei 230009, China

The crystal structure, microstructure, and microwave dielectric properties of forsterite-based $(Mg_{1-x}Ni_x)_2SiO_4$ ($x = 0.02–0.20$) ceramics were systematically investigated. All samples present a single forsterite phase of an orthorhombic structure with a space group Pbnm except for a little $MgSiO_3$ secondary phase as $x > 0.08$. Lattice parameters in all axes decrease linearly with increasing Ni content due to the smaller ionic radius of Ni^{2+} compared to Mg^{2+}. The substitution of an appropriate amount of Ni^{2+} could greatly improve the sintering behavior and produce a uniform and closely packed microstructure of the Mg_2SiO_4 ceramics such that a superior $Q \times f$ value (152 300 GHz) can be achieved as $x = 0.05$. The τ_f value was found to increase with increasing A-site ionic bond valences. In addition, various additives were used as sintering aids to lower the sintering temperature from 1500°C to the middle sintering temperature range. Excellent microwave dielectric properties of $\varepsilon_r \sim 6.9$, $Q \times f \sim 99800$ GHz and $\tau_f \sim -50$ ppm/°C can be obtained for 12 wt% Li_2CO_3-V_2O_5-doped $(Mg_{0.95}Ni_{0.05})_2SiO_4$ ceramics sintered at 1150°C for 4 h.

I. Introduction

MANY superior materials with a complex perovskite or a corundum structure such as $Ba(Zn_{1/3}Ta_{2/3})O_3$,[1] Al_2O_3,[2] $Mg_4Nb_2O_9$[3] have been extensively investigated as candidates for high-frequency applications owing to their low dielectric constant (ε_r) together with high quality factor (Q) values. And search for new low-loss and low-cost dielectric ceramics is always a primary issue in the last few years. In return for many efforts, numerous silicates and titanates including Mg_2SiO_4,[4] Zn_2SiO_4,[5] $MgTiO_3$,[6] and Mg_2TiO_4[7] have been reported to possess a considerably high Q showing a great potential for millimeter-wave applications. Thus, much scientific and commercial attention have been attracted to improve the sinterability and microwave dielectric properties of these compounds by various A- or B-site ionic substitution, for instance, $(Mg_{1-x}M_x)_2SiO_4$ (M=Ca, Mn),[8] $Mg_2(Si_{1-x}Ti_x)O_4$,[9] $(Mg_{1-x}Co_x)_2TiO_4$,[6] $(Mg_{1-x}Mn_x)_2TiO_4$,[10] and $Mg_2(Ti_{1-x}Sn_x)O_4$.[11]

Among these promising materials, forsterite Mg_2SiO_4 ceramics with high performance have been particularly considered because of its low-cost, easily processable, and lightweight characteristics. Its low ε_r of 6.8 and extremely high $Q \times f$ value of 240 000 GHz were first reported by Tsunooka *et al.*[4] However, the metastable enstatite or protoenstatite secondary phases are difficult to be completely eliminated from the Mg_2SiO_4 sample via a mixed-oxide route, which not only result in poor sinterability but also greatly deteriorate the Q value.[12] Some efforts have been made to synthesize pure-phase Mg_2SiO_4 by sol–gel or other wet chemical processes.[13,14] Nevertheless, Song *et al.* still successfully prepared the single-phase Mg_2SiO_4 via the conventional solid-state route by adjusting the Mg/Si ratio.[12] However, it could be noted that the $Q \times f$ values of Mg_2SiO_4 ceramics reported in most prior work[9,12,15,16] are significantly lower than those reported in a previous paper.[4] In addition, some miscellaneous information on $Q \times f$ values for the Mg_2SiO_4 ceramics reported by the same group[4,8] might reflect the strong processing sensitivity of the forsterite ceramics. Recently, it was hypothesized that the temperature coefficient of resonant frequency (τ_f) of the Mg_2SiO_4 ceramic is closely related to the ionic radii of A1 and A2-site cations in the olivine structure, and ions with larger ionic radii and polarizability such as Ca^{2+} and Mn^{2+} tend to bring its τ_f toward minus.[8,17]

Compared to Mg^{2+}, Ni^{2+} can be expected to tailor the τ_f value of the forsterite ceramic owing to its relatively small ionic radius. Particularly, the relation between the microwave dielectric properties and the structure for the Ni^{2+}-doped Mg_2SiO_4 system has not yet been explored from the crystallographic point of view. The experimentally measured microwave dielectric properties were investigated based upon the phase composition, densification, structural characteristics, and microstructures of the ceramics. Moreover, the sintering temperature of $(Mg_{1-x}Ni_x)_2SiO_4$ is considerably high in the currently reported microwave dielectric ceramics. Thus, 12 wt % $2ZnO$-V_2O_5, Li_2CO_3-V_2O_5, Li_2CO_3-B_2O_3, and Li_2CO_3-Bi_2O_3 were used as sintering aids, respectively, to reduce its sintering temperature down to a middle-temperature range.

II. Experimental Procedure

The $(Mg_{1-x}Ni_x)_2SiO_4$ ($x = 0.02–0.20$) ceramics were prepared by a solid-state reaction method using starting materials of high-purity ($\geq 99\%$) oxide powders: $4MgCO_3 \cdot Mg(OH)_2 \cdot 5H_2O$, $C_4H_6O_4Ni \cdot 4H_2O$, and SiO_2 (Sinopharm Chemical Reagent Co. Ltd, Shanghai, China). The powders with the corresponding stoichiometric compositions were ball milled in a nylon jar with zirconia balls on a planetary milling machine (QM-3SP2; NanDa Instrument Plant, Nanjing, China) at 360 rpm for 8 h using distilled water as the media. The slurries were dried at 100°C for 24 h, calcined in air at 1200°C for 3 h, and remilled for 8 h afterward. Subsequently, the obtained mixtures were dried, granulated with 5 wt% PVA in an agate mortar, and then pressed into cylinders of 10 mm in diameter and 5–6 mm in height under a uniaxial pressure of 100 MPa in a stainless-steel die. These samples were first heated at 550°C for 4 h to burn out the organic binder, and then sintered in air at temperatures from 1300°C to 1550°C for 4 h. Moreover, $2ZnO$-V_2O_5, Li_2CO_3-V_2O_5, Li_2CO_3-B_2O_3, and Li_2CO_3-Bi_2O_3 prepared by mixing the corresponding stoichiometric oxides or carbonates in an agate mortar for 3 h were used as the sintering aids to lower the sintering temperatures of the studied materials.

The crystalline structures of the sintered samples were determined by an X-ray diffractometer (XRD; D/Max2500V, Rigaku, Tokyo, Japan) using Cu K_α radiation ($\lambda = 1.5406$ Å) with a step size of 0.01°. The structural parameters were obtained from Rietveld refinement of the XRD data using the FullProf software. The bulk densities of the sintered samples were measured by the Archimedes method. For convenience, the microstructural observation on the natural surface of the sintered samples was performed using a scanning electron microscope (SEM; JEOL JSM-6490LV, Tokyo, Japan) equipped with an energy dispersive spectrometer (EDS). Here, the natural surface refers to the outside surface of the postsintered pellets, instead of the polished and thermally etched surface. A network analyzer (N5230C; Agilent, Palo Alto, CA) and a temperature chamber (GDW-100; Saiweisi, Changzhou, China) were used to measure the dielectric properties of the well-polished ceramic samples with an aspect ratio of 1.8–2.2 in the microwave frequency range by means of Hakki-Coleman post resonator method.[18] The dielectric constants were measured using the parallel conducting plates and the coaxial electric probes as suggested by Courtney at the TE_{011} mode of resonance, which can be least perturbed by the surrounding field variations.[19] For the measurement of the Q value, the sample was placed on the low-loss quartz support of 8 mm diameter and 4 mm height in the center of the cylindrical silver-clad shielded cavity (Resonant cavity; QWED, Warsaw, Poland) with an inner diameter of 32 mm and a height of 18 mm. The loaded quality factor Q_L in transmission mode (S_{21} parameter) was determined from the full-width of the resonance peak at the 3 dB level. The dielectric loss (tanδ) was calculated by using the software provided by the $TE_{01\delta}$-shield cavity supplier, through which the Q values can be obtained in accordance with the equation $Q = 1/tan\delta$. The τ_f value of the samples was measured by noting the change in the resonant frequency over a temperature interval from 25°C to 80°C, and it can be calculated by the following equation:

$$\tau_f = \frac{f_2 - f_1}{f_1(T_2 - T_1)} \tag{1}$$

where f_1 and f_2 represent the resonant frequencies at T_1 and T_2, respectively.

III. Results and Discussion

Figure 1(a) depicts the XRD patterns of $(Mg_{1-x}Ni_x)_2SiO_4$ ($x = 0.02$–0.20) ceramics sintered at 1500°C for 4 h. All the main diffraction peaks can be well indexed in terms of the standard patterns of orthorhombic-structured Mg_2SiO_4 (JCPDS #34-0189), indicating that the forsteritic-olivine solid solution was formed as a single phase. A very little protoenstatite $MgSiO_3$ secondary phase appeared along with the main phase Mg_2SiO_4 in compositions with $x > 0.08$. The possible reason might be ascribed to the fact that the amount of MgO is insufficient so that it could not react with $MgSiO_3$ secondary phase to form Mg_2SiO_4. This result is consistent with a previous report where protoenstatite was easily formed as a by-product when the solid reaction route was used to synthesize the forsterite, because of slow kinetics of the solid-state diffusion.[12] Such impurity phase probably results in poor sinterability of the samples and then extremely degrades the sample's Q value. Furthermore, it can be also found that the intensity of all diffraction peaks have almost no changes except for the peak at ~17° as x value varied. This result is probably ascribed to the occurrence of the preferred grain orientation induced by the Ni substitution.

The detailed structural characteristics of $(Mg_{1-x}Ni_x)_2SiO_4$ ceramics were analyzed using a Rietveld refinement method. The lattice parameters, Wyckoff site, atomic fractional coor-
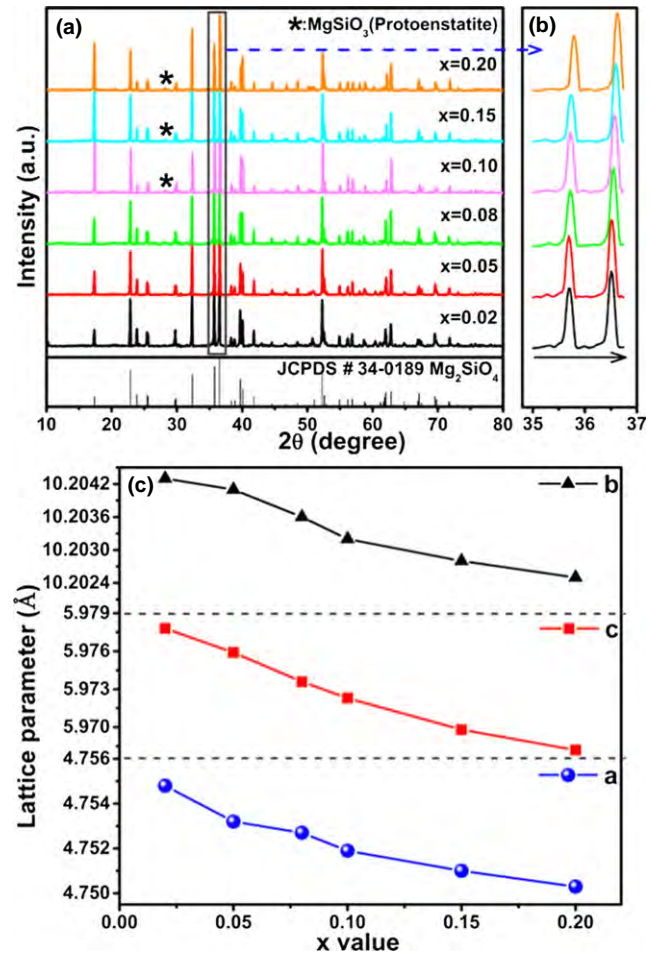

Fig. 1. (a) XRD patterns of $(Mg_{1-x}Ni_x)_2SiO_4$ ($x = 0.02$–0.20) ceramics sintered at 1500°C for 4 h; (b) locally magnified peak profiles indicated in (a); and (c) the lattice parameters as a function of the x value.

dinates and occupancy were initiated by using the Mg_2SiO_4 structural data from the Findit software. In crystallography, the Wyckoff site is one of a set of points for which the site symmetry groups are conjugated subgroups of space group. It was well-known that the olivine is an orthosilicate with a general formula of $A1A2SiO_4$, where both the A1 and A2 sites are 6-coordinated. And the [MgO$_6$] octahedra in forsterite share edges to create chains along the c axis, which have two alternating and distinct types, as shown in Fig. 2(a). The previous studies of X-ray structure refinements, as well as crystal field spectra found that the A1 site is relatively small and flattened along its threefold axis, yet the A2 site is slightly large and is much more distorted.[20] This means the cations with relatively small radii and high octahedral site preference energies, for example, Ni^{2+} and Co^{2+} have a preference for the A1 site. Thus, the occupancy of Ni^{2+} should be allotted for the A1 site of forsterite in the refinement. Simultaneously, the nominal concentration of Ni^{2+} was used to obtain its occupancy. This parameter was not refined because Ni^{2+} could totally dissolve into the Mg_2SiO_4 lattice as confirmed by a previous study.[17] Moreover, the modes used for the calculation of the peak shape and background were Pseudo-Voigt and 6-coefficients polynomial functions, respectively. As the XRD results confirm that samples with $x > 0.08$ contain some impurity phases, a mixture model has been employed for refinement of these samples. The weight fractions of the $MgSiO_3$ impurity phase based on the refined scale factor were found to be 2.53%, 2.76%, and 2.92% corresponding to the $x = 0.10$, 0.15, and 0.20 samples, respectively. The results confirm that the Mg_2SiO_4 phase as
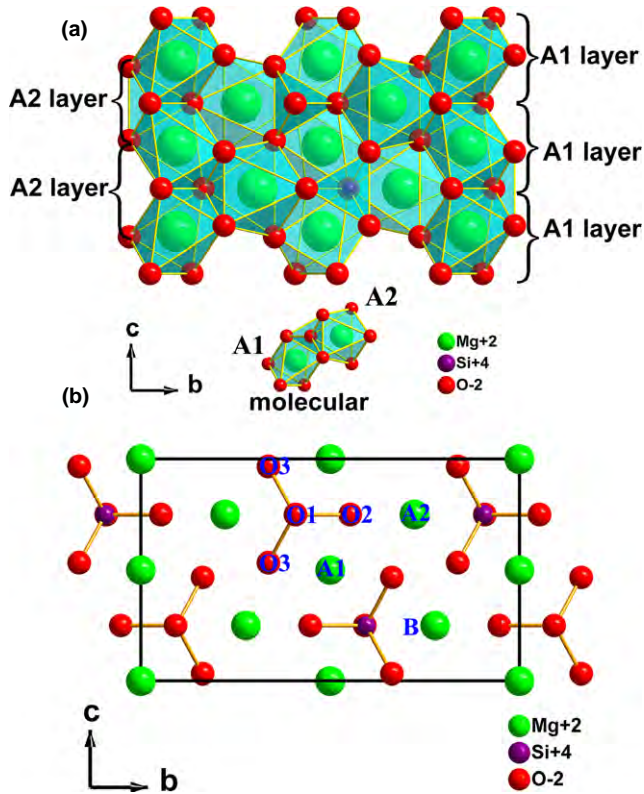
Fig. 2. (a) Crystal structure of forsterite Mg_2SiO_4 observed along the [100] orientation, and (b) the projection drawing of forsterite Mg_2SiO_4 on (100) plane.

well as $MgSiO_3$ phase shows an orthorhombic structure and a wollastonite structure, respectively. The refined lattice parameters and unit cell volumes of Mg_2SiO_4 ceramics, reliability factors and goodness-of-fit indicator are presented in Table I. All the refinement results with the pattern R factor (R_p) range from 5% to 11%, the weighted pattern R factor (R_{wp}) range from 8% to 13% and the goodness of fit indicator (χ^2) range from 1.4 to 1.8, suggest that the structural model is valid. With increasing the Ni content, both the lattice parameters and unit cell volumes slightly decrease as a consequence of the substitution of smaller Ni^{2+} (0.69 Å, CN=6) for Mg^{2+} (0.72 Å, CN=6). This result is in good agreement with that the diffraction peak shift of the forsterite phase toward to higher angles in XRD patterns, as shown in Fig. 1(b). Moreover, the refined lattice parameters were also plotted as a function of x value as shown in Fig. 1(c). A nearly linear dependence between the lattice parameters and x value can be found, which is consistent with the Vegard's law, and also confirms the formation of a solid solution.

To investigate the relationship between the grain morphological changes and the composition as well as the sintering temperature of the samples, the natural surface microstructure of the $(Mg_{1-x}Ni_x)_2SiO_4$ ($x = 0.02–0.20$) ceramics sintered

at various temperatures was observed, as shown in Fig. 3. It can be noted from Figs. 3(a)–(d) that the grains grow extremely well and are closely packed with almost no pores, instead of inhomogeneous microstructures as previously reported,[4,8,9,12] indicating that a small amount of Ni substitution could significantly improve the densification behavior of the Mg_2SiO_4 ceramics. The majority of the grains have an average size of 1–3 μm. With increasing x, the grain size slightly increases. At the same time, the grain morphology changes from planar to cobbly morphology, and a small amount of pores appear in $x = 0.15$ and 0.20 samples [Figs. 3(e) and (f)]. Especially, it is interesting to note that some small grains indicated by white arrows emerge at the grain boundaries in the samples with $x = 0.15$ and 0.20, probably because a number of the abnormal grains impinged upon each other during early stages of grain growth. In addition, the grain boundaries seem to melt in the sample with $x = 0.20$ sintered at 1500°C [Fig. 3(f)]. These results can be responsible for the fact that a small amount of Ni substitution to some extent lowered the sintering temperature of the samples, and mild oversintering behavior occurred in the samples with $x = 0.15$ and 0.20 sintered at 1500°C, which in turn probably degrades the $Q \times f$ values of the samples. On the other hand, with increasing sintering temperature, the average grain size of the $(Mg_{0.95}Ni_{0.05})_2SiO_4$ sample increases with an enhancement in compactness and uniformity of the microstructure [Figs. 3(b), (g), and (h)]. The enhanced grain growth behavior tends to lower the sintering driving force for densification and inhibit extraction of pores from green bodies, so that the sample density decreases and grains grow abnormally as the sintering temperature is too high [Fig. 3(h)]. Therefore, the most dense and uniform microstructure was achieved in the sample with $x = 0.05$ sintered at 1500°C, which is directly beneficial to the microwave dielectric properties of the samples.

The relative densities and ε_r values of $(Mg_{1-x}Ni_x)_2SiO_4$ ceramics as a function of the sintering temperature are offered in Fig. 4. The relative densities in percentage stand for the ratios of the measured densities to the theoretical densities. At first, the theoretical densities of the solid solution samples ($x \leq 0.08$) and the composite samples ($x > 0.08$) were calculated using the Eqs. 2 and 3, respectively:

$$\rho_{theo} = \frac{ZM}{N_A V_{unit}} \tag{2}$$

$$\rho = \frac{\omega_1 + \omega_2}{\omega_1/\rho_1 + \omega_2/\rho_2} \tag{3}$$

where Z is the number of atoms per unit cell, M is the molar weight (g/mol), N_A is the Avogadro number (6.023×10^{23} atoms per mol), and V_{unit} is the volume of the unit cell (in cm^3),[21] ρ_1 and ρ_2 are the theoretical densities of Mg_2SiO_4 and $MgSiO_3$ (2.911 g/cm^3 for Mg_2SiO_4 pure-phase and 3.101 g/cm^3 for $MgSiO_3$ pure-phase),[12,22] ω_1 and ω_2 are the

Table I. Refined Lattice Parameters (a, b, and c) and Unit Cell Volume (V_{unit}) of $(Mg_{1-x}Ni_x)_2SiO_4$ ($x = 0.02–0.20$) Ceramics Sintered at 1500°C for 4 h

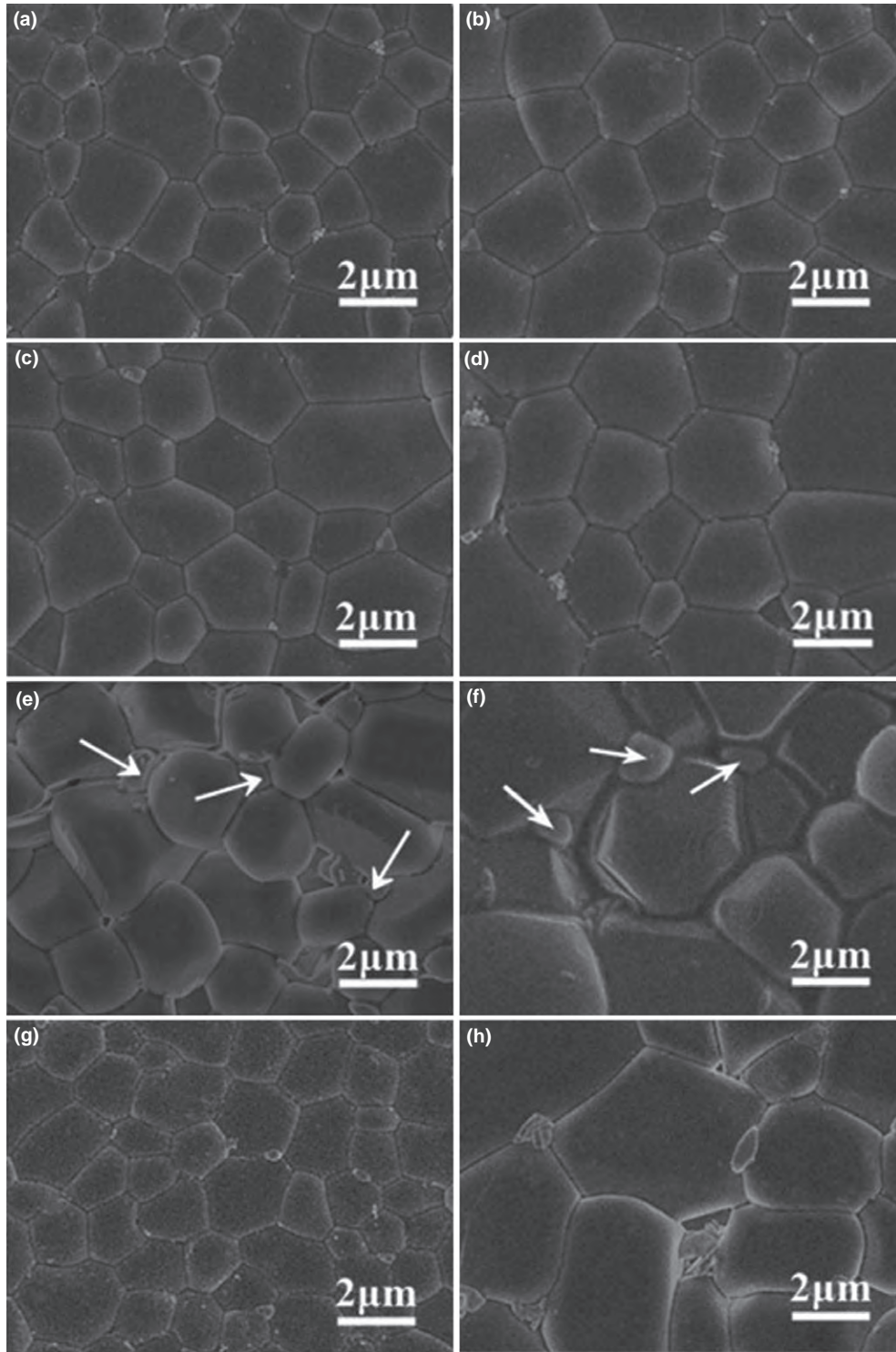| Ni Content (x)	a (Å)	b (Å)	c (Å)	V_{unit} (Å)	R_{wp}(%)	R_p(%)	χ^2
0.02	4.7548(6)	10.2043(4)	5.9778(5)	289.68(1)	9.79	7.06	1.547
0.05	4.7532(4)	10.2041(1)	5.9759(8)	289.536(7)	8.45	5.61	1.426
0.08	4.7527(3)	10.2036(2)	5.9736(7)	289.478(6)	11.4	9.42	1.656
0.10	4.7519(2)	10.2032(3)	5.9723(8)	289.448(6)	12.3	10.6	1.741
0.15	4.7510(2)	10.2028(2)	5.9698(4)	289.365(3)	9.13	6.58	1.469
0.20	4.7503(1)	10.2025(4)	5.9682(3)	289.251(2)	8.83	6.14	1.473

Fig. 3. SEM micrographs of (Mg$_{1-x}$Ni$_x$)$_2$SiO$_4$ ceramics sintered at 1500°C for 4 h: (a) $x = 0.02$, (b) $x = 0.05$, (c) $x = 0.08$, (d) $x = 0.10$, (e) $x = 0.15$, (f) $x = 0.20$, and (Mg$_{0.95}$Ni$_{0.05}$)$_2$SiO$_4$ ceramics sintered at different temperatures for 4 h: (g) 1450°C, (h) 1550°C.

weight fractions of Mg$_2$SiO$_4$ and MgSiO$_3$, respectively. For all samples, with increasing the sintering temperature, the relative densities gradually increase up to 1500°C and then reach a maximum value, which is due to the grain growth and the decrease in pores (whose ε_r near to 1), as shown in Figs. 3(b) and (g). The relative densities decline afterward, suggesting that 1500°C would be the optimized sintering temperature. Of note is that the sample with $x = 0.05$ has the highest relative density of 97.5% compared to other compositions, which can be attributed to the reduction in porosity,

the increase in average grain size and its relatively uniform microstructure [Fig. 3(b)].

Generally, the ε_r is dependent on the ionic polarizabilities of the composition, relative density and secondary phase. The variation in ε_r exhibits almost a similar behavior to that of relative density with the sintering temperature. To evaluate the relative error in the measurement of ε_r, we have calculated the observed polarizability (α_{obs}) and the theoretical ε_r (ε_{theo}) by the Clausius–Mosotti relation,[23] as defined in Eqs. (4) and (5):
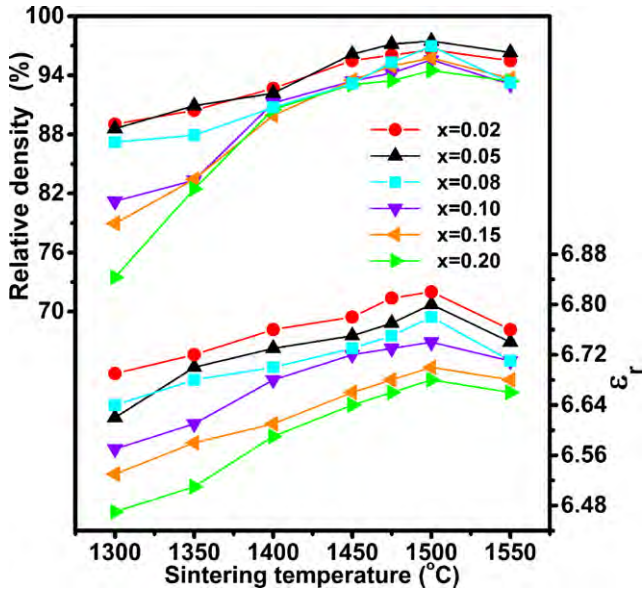
Fig. 4. Relative densities and ε_r values of $(Mg_{1-x}Ni_x)_2SiO_4$ ($x = 0.02$–0.20) ceramics sintered at different temperatures for 4 h.

Fig. 5. The $Q \times f$ values of $(Mg_{1-x}Ni_x)_2SiO_4$ ($x = 0.02$–0.20) ceramics sintered at different temperatures for 4 h; the inset shows the τ_f values of $(Mg_{1-x}Ni_x)_2SiO_4$ ceramics as a function of A-site bond valences.

$$\alpha_{obs} = \frac{V_m(\varepsilon_{obs} - 1)}{b(\varepsilon_{obs} + 2)} \quad (4)$$

$$\varepsilon_{theo} = \frac{3}{1 - b\alpha_{theo}/V_m} - 2 \quad (5)$$

where b is defined as $4\pi/3$, ε_{obs} is the dielectric constant measured, V_m is the molecular volume, and α_{theo} is the sum of theoretical ionic polarizability (Mg^{2+}: 1.32 Å^3, Ni^{2+}: 1.23 Å^3, Si^{4+}: 0.87 Å^3, O^{2-}: 2.01 Å^3).[24] All data involved are listed in Table II. It can be seen that all the values of ε_{theo}, ε_{obs}, α_{theo} and α_{obs} have an agreeable trend of decreasing with the Ni content increasing. The ε_{obs} value decreases from 6.82 to 6.68 with increasing x due to the smaller ionic polarizability of Ni^{2+} (1.23 Å^3) than that of Mg^{2+} (1.32 Å^3), as well as the smaller ε_r of $MgSiO_3$ (6.45) than that of Mg_2SiO_4 (6.8).[4,22] In addition, a certain deviation between the theoretical and the experimental results exists, and is correlated with the relative density.

Figure 5 displays the $Q \times f$ values of $(Mg_{1-x}Ni_x)_2SiO_4$ ceramics as a function of the sintering temperature. The microwave dielectric loss is not only related to the intrinsic loss such as the lattice vibrational modes, but also is closely associated with extrinsic losses such as porosity, grain boundaries, microcracks, secondary phases, and impurities.[25] The variation of $Q \times f$ shows a similar trend to that of the relative density, which reflects that the dielectric loss was mainly dominated by the densification of the ceramics. It is noteworthy that a marked enhancement of
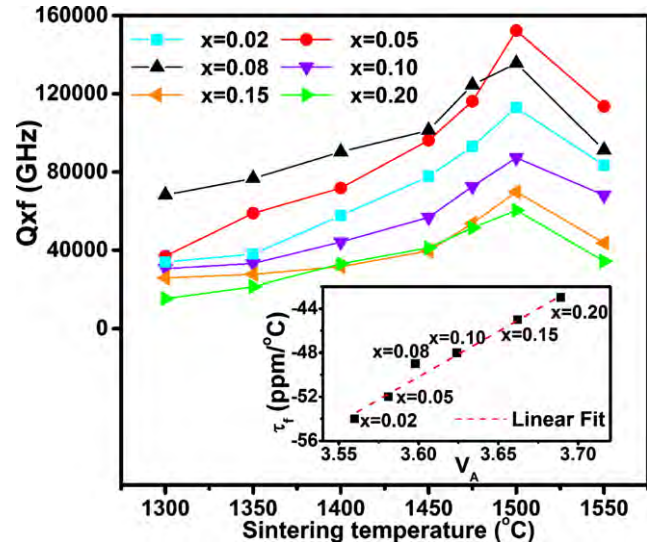
the $Q \times f$ value (96 180–152 300 GHz) appears in $(Mg_{0.95}Ni_{0.05})_2SiO_4$ samples with increasing the sintering temperature from 1450°C to 1500°C. This might be by virtue of the grain growth and the reduction in grain boundaries [Figs. 3(b) and (g)], which usually act as sinks for the accumulation of the impurities during the sintering process and thus have a deleterious influence on the extrinsic loss. Then the $Q \times f$ value decreases with further increase of the sintering temperature because of the nonuniform and abnormal grain growth, as shown in Fig. 3(h). In addition, for samples with $x > 0.08$, the overall $Q \times f$ values were lower than those of the samples with less x, probably due in large part to the appearance of $MgSiO_3$ phase, whose $Q \times f$ value was reported to be about 60 000 GHz.[22] Thus, a maximum $Q \times f$ value of 152 300 GHz could be achieved for the samples of $(Mg_{0.95}Ni_{0.05})_2SiO_4$ sintered at 1500°C for 4 h. This result indicates that a superior $Q \times f$ value can be obtained in Mg_2SiO_4 ceramics by an appropriate substitution, as already shown in other solid solutions.[6,10,26,27]

Another important dielectric property for microwave applications is τ_f, which determines the thermal stability of materials and devices. The τ_f of materials basically results from the τ_ε related to the chemical nature of constituent ions, the distance between cations and anions and the structural characteristics originating from the bonding type. These structural characteristics could be evaluated by the bond valence of ions. The bond valence V_{ij} of atom i, was defined as the sum of all of the valences from a given atom i, and could be calculated by Eqs. (6) and (7):[28]

Table II. Comparison of Theoretical and Observed Polarizabilities, as well as Dielectric Constants of $(Mg_{1-x}Ni_x)_2SiO_4$ ($x = 0.02$–0.20) Ceramics Sintered at 1500°C for 4 h

Ni Content (x)	Theoretical		Observed				$\Delta\%$	
	α_{theo}	ε_{theo}	ε_{obs}	V_{unit} (Å)	Z	α_{obs}	$(\alpha_{obs} - \alpha_{theo})/\alpha_{obs} \times 100$	$(\varepsilon_{obs} - \varepsilon_{theo})/\varepsilon_{obs} \times 100$
0.02	11.5464	7.0321	6.82	289.6774	4	11.4083	−1.211	−3.110
0.05	11.5410	7.0325	6.80	289.5360	4	11.3692	−1.331	−3.877
0.08	11.5356	7.0277	6.77	289.4779	4	11.3534	−1.484	−4.113
0.10	11.5320	7.0239	6.74	289.4482	4	11.3455	−1.644	−4.231
0.15	11.5230	7.0149	6.70	289.3651	4	11.3150	−1.839	−4.700
0.20	11.5140	7.0079	6.68	289.2510	4	11.2968	−1.923	−4.909

$$v_{ij} = \exp[\frac{R_{ij} - d_{ij}}{b'}] \qquad (6)$$

$$V_{ij} = \Sigma v_{ij} \qquad (7)$$

where R_{ij} is the bond valence parameter, d_{ij} is the length of a bond between atom i and j, and b' is commonly taken to be a universal constant equal to 0.37 Å. It has been reported[29] that the τ_f of a complex perovskite would decrease as the bond valence of the A-site decreased, owing to the tilting of the oxygen octahedra induced by the smaller ionic radius of the A site. The same phenomenon has also been shown in tetragonal scheelite structures and monoclinic-structured $Zn_3Nb_2O_8$ ceramics.[26,28] In this study, the bond lengths were calculated using the Bond_Str program (FullProf suite 2.05) and the results are listed in Table III, together with the projection drawing of the forsterite Mg_2SiO_4 on (100) plane illustrated in Fig. 2(b). With an increase in the Ni content, the bond valence of the A-site increased. The τ_f values of the $(Mg_{1-x}Ni_x)_2SiO_4$ ceramics as a function of A-site bond valence are provided in the inset of Fig. 5. With the increase in A-site bond valence, the average bond strength of A-site ions could be decreased. This in turn, would decrease the degree of distortion of oxygen octahedra. As a result, the temperature coefficient of the dielectric constant decreased and finally τ_f would thereupon increase.[30] In addition, the improvement of the τ_f for the samples with $x > 0.08$, might be also caused by the emergence of $MgSiO_3$ secondary phase, whose τ_f is around −44 ppm/°C.[22]

In addition to the microwave dielectric properties, the low-temperature sinterability of materials should be another significant merit in electronic industry for microwave applications. To the best of our knowledge, only a few studies have been conducted to lower the sintering temperature of forsterite-based ceramics. Sebastian *et al.* have reported that addition of 15 wt% lithium borosilicate or lithium magnesium zinc borosilicate could lower the sintering temperature of forsterite ceramics from 1500°C to about 950°C, resulting in the $Q \times f$ values of approximately 30 000 GHz.[31,32] Thus, in this study, we attempt to use four low-melting additives including $2ZnO-V_2O_5$, $Li_2CO_3-V_2O_5$, $Li_2CO_3-B_2O_3$, and $Li_2CO_3-Bi_2O_3$ to lower the sintering temperature of $(Mg_{0.95}Ni_{0.05})_2SiO_4$ ceramics. It was found that controlling the additive dosage at 12 wt% could not only effectively lower the sintering temperature, but also maintain excellent $Q \times f$ values of the samples. Figure 6 shows the XRD patterns of $(Mg_{0.95}Ni_{0.05})_2SiO_4$ ceramics doped with various additives sintered at 1150°C for 4 h. A homogeneous $(Mg_{0.95}Ni_{0.05})_2SiO_4$ phase was classified as the main crystal phase; however, a small amount of other impurity phases were detected in all samples. This result reveals that Zn, Li, V, and B containing sintering aids are easily to react with the matrix during the
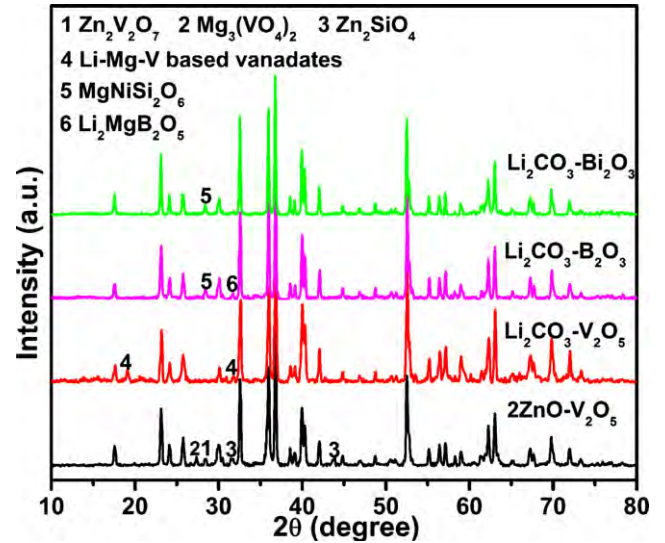

Fig. 6. XRD patterns of $(Mg_{0.95}Ni_{0.05})_2SiO_4$ ceramics doped with 12 wt% sintering aids sintered at 1150°C for 4 h.

sintering process, and would probably affect the sintering behavior and microwave dielectric properties of the matrix ceramics.

Figure 7(a) illustrates the apparent densities of the $(Mg_{0.95}Ni_{0.05})_2SiO_4$ ceramics doped with 12 wt% additives sintered at different temperatures. With increasing sintering temperature, the apparent density of the samples increases to a maximum value and decreases thereafter. The samples with 12 wt% $Li_2CO_3-V_2O_5$ could achieve the highest density of approximately 3.4 g/cm^3 at about 1150°C. It can be noted that the variation in the apparent density is remarkable for all four samples, indicating that the sintering window of the $(Mg_{0.95}Ni_{0.05})_2SiO_4$ ceramics with additives is rather narrow. Moreover, the addition of 12 wt% $2ZnO-V_2O_5$, $Li_2CO_3-V_2O_5$, or $Li_2CO_3-Bi_2O_3$ could effectively lower the sintering temperature to 1150°C, however, the addition of 12 wt% $Li_2CO_3-B_2O_3$ could only reduce it to 1250°C. The SEM micrographs of the natural surface of these samples sintered at their optimized temperatures are also offered in Figs. 7(b)–(e). It can be observed that the sample's surface morphology changed obviously from planar grains [Fig. 3(b)] to virgulate and massy grains [Figs. 7(b)–(e)]. Furthermore, a bimodal grain size distribution appears in all samples, and the EDS analysis was carried out to identify the compositions of different grains, as shown in Figs. 7(f) and (g). The results demonstrated that both small and large grains [marked S and L in Figs. 7(b)–(e), respectively] consist of Si, Mg, Ni, and O elements in an approximate molar ratio of Si:

Table III. The Effective Bond Valence Parameter, Length of Bonds, and A-site Bond Valence of $(Mg_{1-x}Ni_x)_2SiO_4$ (x = 0.02–0.20) Ceramics Sintered at 1500°C for 4 h

|		$x = 0.02$	$x = 0.05$	$x = 0.08$	$x = 0.10$	$x = 0.15$	$x = 0.20$
R_{A-O}		1.6922	1.6911	1.6899	1.6891	1.6872	1.6852
2-d(A1–	O1)	2.1237	2.1213	2.1195	2.1174	2.1122	2.1085
	O2)	2.1045	2.0981	2.0940	2.0876	2.0756	2.0681
	O3)	2.1698	2.1679	2.1661	2.1639	2.1603	2.1574
d(A2–	O1)	2.2581	2.2555	2.2533	2.2509	2.2473	2.2448
	O2)	2.0803	2.0780	2.0755	2.0732	2.0688	2.0664
	O3)	2.2794	2.2721	2.2671	2.2625	2.2577	2.2503
	O3)	2.0531	2.0520	2.0489	2.0459	2.0416	2.0374
	O3)	2.0531	2.0520	2.0489	2.0459	2.0416	2.0374
	O3)	2.2794	2.2721	2.2671	2.2625	2.2577	2.2503
V_{A-O}		3.5598	3.5809	3.5983	3.6242	3.6625	3.6893
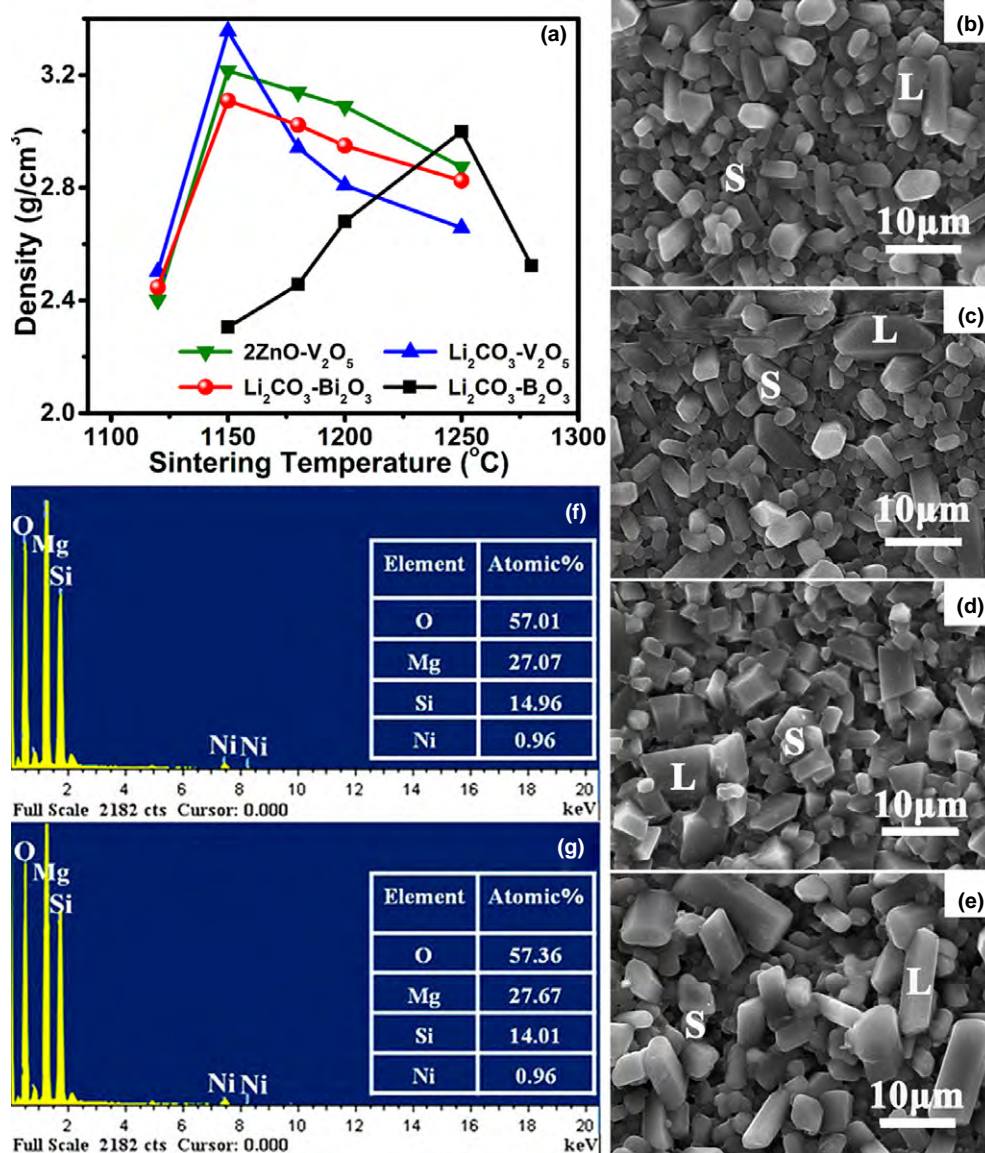
Fig. 7. (a) Densities of $(Mg_{0.95}Ni_{0.05})_2SiO_4$ ceramics with 12 wt% various additives as a function of sintering temperatures; (b)–(e) SEM micrographs on the natural surface of these samples doped with 12 wt% $2ZnO-V_2O_5$, $Li_2CO_3-V_2O_5$, $Li_2CO_3-B_2O_3$, and $Li_2CO_3-Bi_2O_3$ sintered at optimized temperatures, respectively; (f) and (g) EDS results of small and large grains in the above-mentioned samples as indicated in (b)–(e), respectively.

Mg:Ni:O = 10:19:1:40, suggesting that both small and large grains belong to the $(Mg_{0.95}Ni_{0.05})_2SiO_4$ phase.

The microwave dielectric properties of $(Mg_{0.95}Ni_{0.05})_2SiO_4$ ceramics doped with 12 wt% additives as a function of the sintering temperature are depicted in Fig. 8. The variation of both ε_r and $Q \times f$ values was consistent with the change of the sample density. The ε_r value of the samples with 12 wt% $Li_2CO_3-V_2O_5$, $Li_2CO_3-B_2O_3$, and $Li_2CO_3-Bi_2O_3$ is approximately in the range 6.4–6.86, which is roughly similar to that of the matrix phase ($\varepsilon_r = 6.8$). The decreased ε_r might be related to the decreased densities. For the samples with 12 wt% $2ZnO-V_2O_5$, both increased ε_r (7.2–7.5) and decreased τ_f (~−75 ppm/°C) should be mainly ascribed to the presence of some $Zn_2V_2O_7$, $Mg_3(VO_4)_2$ and Zn_2SiO_4 phases, because both $Mg_3(VO_4)_2$ (ε_r~9.3, τ_f~89.5 ppm/°C)[33] and Zn_2SiO_4 (ε_r~6.6, τ_f~−61 ppm/°C)[5] show larger ε_r and smaller τ_f values. According to our previous work,[25] the $Zn_2V_2O_7$ can be formed by the decomposition of the $Zn_3(VO_4)_2$ phase as sintering temperature exceeds 815°C and it has similar ε_r and τ_f values to those of $Zn_3(VO_4)_2$ (ε_r~10, τ_f~−120 ppm/°C). Despite the content of these secondary phases would be very low, the τ_f value of the ceramics was obviously reduced.

In addition, all samples exhibited considerably low $Q \times f$ values (66 700–99 800 GHz) compared to that of the matrix phase (152 300 GHz), owing mostly likely to both the presence of various secondary phases and relatively low densities. Nevertheless, the $(Mg_{0.95}Ni_{0.05})_2SiO_4$ ceramics with 12 wt% $Li_2CO_3-V_2O_5$ sintered at 1150°C for 4 h attain a low ε_r value of 6.9, an excellent $Q \times f$ value of 99 800 GHz and a τ_f value of −50 ppm/°C, probably being a potential candidate for microwave dielectric substrate applications.

IV. Conclusions

The microwave dielectric properties of forsterite-based $(Mg_{1-x}Ni_x)_2SiO_4$ ($x = 0.02$–0.20) ceramics were investigated in terms of their structural characteristics, microstructure, as well as the sintering behavior. The results demonstrate that the Ni substitution not only significantly boosts the densification behavior but also improves the microwave dielectric properties of the ceramics. The τ_f value of the samples was found to increase with increasing the A-site bond valence. A low ε_r of 6.8 and a high $Q \times f$ value of 152 300 GHz can be achieved in the $(Mg_{0.95}Ni_{0.05})_2SiO_4$ sample. In addition,

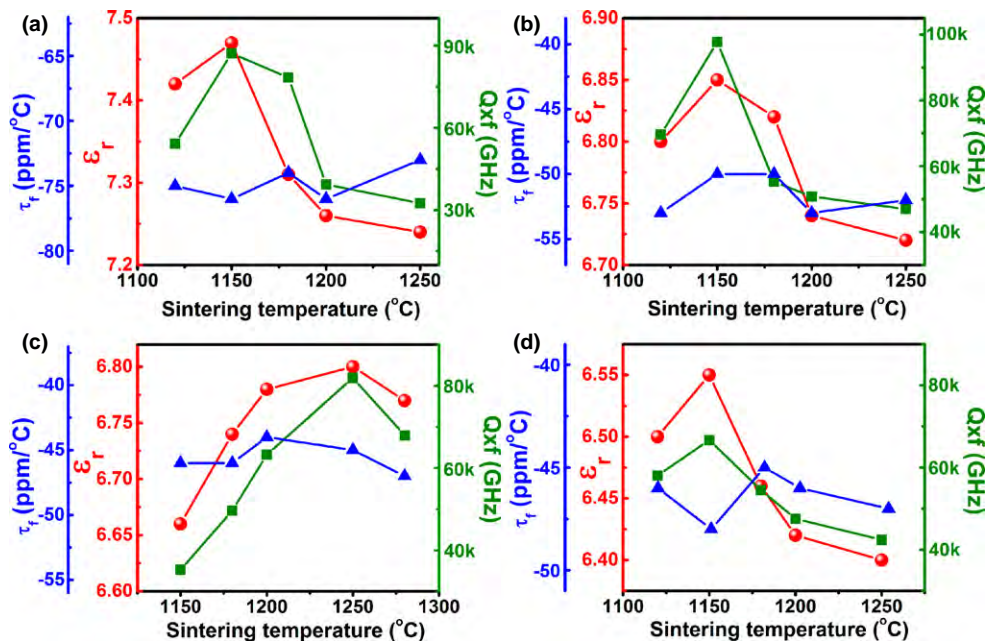**Fig. 8.** Microwave dielectric properties of $(Mg_{0.95}Ni_{0.05})_2SiO_4$ ceramics with 12 wt% (a) $2ZnO-V_2O_5$, (b) $Li_2CO_3-V_2O_5$, (c) $Li_2CO_3-B_2O_3$, and (d) $Li_2CO_3-Bi_2O_3$ additives sintered at different temperatures for 4 h.

four different additives were used as sintering aids to lower its sintering temperature from 1500°C down to the middle sintering temperature range. The $(Mg_{0.95}Ni_{0.05})_2SiO_4$ ceramics with 12 wt% $Li_2CO_3-V_2O_5$ sintered at 1150°C for 4 h achieved excellent microwave dielectric properties of $\varepsilon_r\sim6.9$, $Q \times f\sim99\ 800$ GHz and $\tau_f\sim-50$ ppm/°C, indicating possible materials for millimeter-wave device applications.

Acknowledgments

References

[1]S. Kawashima, M. Nishida, I. Ueda, and H. Ouchi, "Ba(Zn₁/₃Ta₂/₃)O₃ Ceramics With Low Dielectric Loss at Microwave-Frequencies," *J. Am. Ceram. Soc.*, **66**, 421–3 (1983).

[2]N. Mc, N. Alford, and S. J. Penn, "Sintered Alumina With Low Dielectric Loss," *J. Appl. Phys.*, **80**, 5895–8 (1996).

[3]A. Kan, H. Ogawa, A. Yokoi, and Y. Nakamura, "Crystal Structure Refinement of Corundum-Structured $A_4M_2O_9$ (A=Co and Mg, M=Nb and Ta) Microwave Dielectric Ceramics by High-Temperature X-ray Powder Diffraction," *J. Eur. Ceram. Soc.*, **27**, 2977–81 (2007).

[4]T. Tsunooka, M. Androu, Y. Higashida, H. Sugiura, and H. Ohsato, "Effects of TiO₂ on Sinterability and Dielectric Properties of High-Q Forsterite Ceramics," *J. Eur. Ceram. Soc.*, **23**, 2573–8 (2003).

[5]Y. P. Guo, H. Ohsato, and K. Kakimoto, "Characterization and Dielectric Behavior of Willemite and TiO₂-Doped Willemite Ceramics at Millimeter-Wave Frequency," *J. Eur. Ceram. Soc.*, **26**, 1827–30 (2006).

[6]C. L. Huang and J. Y. Chen, "High-Q Microwave Dielectrics in the $(Mg_{1-x}Co_x)_2TiO_4$ Ceramics," *J. Am. Ceram. Soc.*, **92**, 379–83 (2009).

[7]A. Belous, O. Ovchar, D. Durilin, M. M. Krzmanc, M. Valant, and D. Suvorov, "High-Q Microwave Dielectric Materials Based on the Spinel Mg₂TiO₄," *J. Am. Ceram. Soc.*, **89**, 3441–5 (2006).

[8]T. Sugiyama, T. Tsunooka, K. Kakimoto, and H. Ohsato, "Microwave Dielectric Properties of Forsterite-Based Solid Solutions," *J. Eur. Ceram. Soc.*, **26**, 2097–106 (2006).

[9]K. X. Song and X. M. Chen, "Phase Evolution and Microwave Dielectric Characteristics of Ti-Substituted Mg₂SiO₄ Forsterite Ceramics," *Mater. Lett.*, **62**, 520–2 (2008).

[10]C. L. Huang and J. Y. Chen, "Low-Loss Microwave Dielectric Ceramics Using $(Mg_{1-x}Mn_x)_2TiO_4$ (x = 0.02–0.1) Solid Solution," *J. Am. Ceram. Soc.*, **92**, 675–8 (2009).

[11]C. L. Huang and J. Y. Chen, "Low-Loss Microwave Dielectrics Using Mg₂(Ti₁₋ₓSnₓ)O₄ (x = 0.01–0.09) Solid Solution," *J. Am. Ceram. Soc.*, **92**, 2237–41 (2009).

[12]K. X. Song, X. M. Chen, and X. C. Fan, "Effect of Mg/Si Ratio on Microwave Dielectric Characteristics of Forsterite Ceramics," *J. Am. Ceram. Soc.*, **90**, 1808–11 (2007).

[13]D. G. Park, M. Hogan, E. Martin, C. K. Ober, and J. M. Burlitch, "Crystallization of Precursors to Forsterite and Chromium-Doped Forsterite," *J. Am. Ceram. Soc.*, **77**, 33–40 (1994).

[14]A. Kazakos, S. Koarneni, and R. Roy, "Preparation and Densification of Forsterite (Mg₂SiO₄) by Nanocomposite Sol-Gel Processing," *Mater. Lett.*, **10**, 405–9 (1990).

[15]I. H. Park, B. S. Kim, K. Y. Kim, and B. H. Kim, "Microwave Dielectric Properties and Mixture Behavior of CaWO₄-Mg₂SiO₄ Ceramics," *Jpn. J. Appl. Phys.*, **40**, 4956–60 (2001).

[16]K. X. Song, X. M. Chen, and C. W. Zheng, "Microwave Dielectric Characteristics of Ceramics in Mg₂SiO₄-Zn₂SiO₄ System," *Ceram. Inter.*, **34**, 917–20 (2008).

[17]T. Sugiyama, H. Ohsato, T. Tsunooka, and K. Kakimoto, "Effect of Ionic Radii and Polarizability on the Microwave Dielectric Properties of Forsterite Solid Solutions," *Adv. Electron. Ceram. Mater*, **26**, 155–60 (2008).

[18]B. W. Hakki and P. D. Coleman, "A Dielectric Resonant Method of Measuring Inductive Capacitance in the Millimeter Range," *IEEE Trans. Microwave Theory Tech.*, **8**, 402–10 (1960).

[19]W. E. Courtney, "Analysis and Evaluation of a Method of Measuring the Complex Permittivity and Permeability of Microwave Insulators," *IEEE Trans. Microwave Theory Tech*, **18**, 476–85 (1970).

[20]M. D. Dyar, E. C. Sklute, O. N. Menzies, P. A. Bland, D. Lindsley, T. Glotch, M. D. Lane, M. W. Schaefer, B. Wopenka, R. Klima, J. L. Bishop, T. Hiroi, C. Pieters, and J. Sunshine, "Spectroscopic Characteristics of Synthetic Olivine: An Integrated Multi-Wavelength and Multi-Technique Approach," *Am. Mineral.*, **94**, 883–98 (2009).

[21]T. S. Kumar, P. Gogoi, A. Perumal, P. Sharma, and D. Pamu, "Effect of Cobalt Doping on the Structural, Microstructure and Microwave Dielectric Properties of MgTiO₃ Ceramics Prepared by Semi Alkoxide Precursor Method," *J. Am. Ceram. Soc.*, **97**, 1054–9 (2014).

[22]Q. L. Zhang, H. Yang, and H. P. Sun, "A New Microwave Ceramic With Low-Permittivity for LTCC Applications," *J. Eur. Ceram. Soc.*, **28**, 605–9 (2008).

[23]P. Zhang, Z. K. Song, Y. Wang, and L. X. Li, "Effect of Ion Substitution for Nd³⁺ Based on Structural Characteristics on the Microwave Dielectric Properties of NdNbO₄ Ceramic System," *J. Am. Ceram. Soc.*, **97**, 976–81 (2014).

[24]R. D. Shannon, "Dielectric Polarizabilities of Ions in Oxides and Fluorides," *J. Appl. Phys.*, **73**, 348–66 (1960).

[25]Y. Lv, R. Z. Zuo, Y. Cheng, and C. Zhang, "Low-Temperature Sinterable (1–x)Ba₃(VO₄)₂-XLiMg₀.₉Zn₀.₁PO₄ Microwave Dielectric Ceramics," *J. Am. Ceram. Soc.*, **96**, 3862–7 (2013).

[26]C. L. Huang, W. R. Yang, and P. C. Yu, "High-Q Microwave Dielectrics in Low-Temperature Sintered (Zn₁₋ₓNiₓ)₃Nb₂O₈ Ceramics," *J. Eur. Ceram. Soc.*, **34**, 277–84 (2014).

[27]C. L. Huang, C. H. Su, and C. M. Chang, "High-Q Microwave Dielectric Ceramics in the Li₂(Zn₁₋ₓAₓ)Ti₃O₈ (A=Mg, Co; x = 0.02–0.1) System," *J. Am. Ceram. Soc.*, **94**, 4146–9 (2011).

[28]E. S. Kim, B. S. Chun, R. Freer, and R. J. Cernik, "Effects of Packing Fraction and Bond Valence on Microwave Dielectric Properties of $A^{2+}B^{6+}O_4$ (A^{2+}: Ca, Pb, Ba; B^{6+}: Mo, W) Ceramics," *J. Eur. Ceram. Soc.*, **30**, 1731–6 (2010).

[29]H. S. Park, K. H. Yoon, and E. S. Kim, "Effect of Bond Valence on Microwave Dielectric Properties of Complex Perovskite Ceramics," *Mater. Chem. Phys.*, **79**, 181–3 (2003).

[30]C. F. Tseng, P. J. Tseng, C. M. Chang, and Y. C. Kao, "Novel Temperature Stable Li_2MnO_3 Dielectric Ceramics With High Q for LTCC Applications," *J. Am. Ceram. Soc.*, **97**, 1918–22 (2014).

[31]T. S. Sasikala, M. N. Suma, P. Mshanan, C. Pavithran, and M. T. Sebastian, "Forsterite-Based Ceramic-Glass Composites for Substrate Applications in Microwave and Millimeter Wave Communications," *J. Alloy. Compd.*, **461**, 555–9 (2008).

[32]T. S. Sasikala, C. Pavithran, and M. T. Sebastian, "Effect of Lithium Magnesium Zinc Borosilicate Glass Addition on Densification Temperature and Dielectric Properties of Mg_2SiO_4 Ceramics," *J. Mater. Sci.: Mater. Electron.*, **21**, 141–4 (2010).

[33]R. Umemura, H. Ogawa, and A. Kan, "Low Temperature Sintering and Microwave Dielectric Properties of $(Mg_{3-x}Zn_x)(VO_4)_2$ Ceramics," *J. Eur. Ceram. Soc.*, **26**, 2063–8 (2006). □